Bioorganic Chemistry 111 (2021) 104823

Contents lists available at ScienceDirect

Bioorganic Chemistry

journal homepage: www.elsevier.com/locate/bioorg

New benzimidazolequinones as trypanosomicidal agents

Claudia López-Lira [a], Ricardo A. Tapia [a,*], Alejandra Herrera [b], Michel Lapier [b], Juan D. Maya [b], Jorge Soto-Delgado [c,*], Allen G. Oliver [d], A. Graham Lappin [d], Eugenio Uriarte [e]

[a] Facultad de Química y de Farmacia, Pontificia Universidad Católica de Chile, Santiago 6094411, Chile
[b] Instituto de Ciencias Biomédicas (ICBM), Facultad de Medicina, Universidad de Chile, Santiago 8380453, Chile
[c] Departamento de Ciencias Químicas, Facultad de Ciencias Exactas, Universidad Andrés Bello, Viña del Mar 2531015, Chile
[d] Department of Chemistry and Biochemistry, University of Notre Dame, Notre Dame, IN 46556, United States
[e] Departamento de Química Orgánica, Facultad de Farmacia, Universidad Santiago de Compostela, 15782 Santiago de Compostela, Spain

ARTICLE INFO

Keywords:
Aryloxyquinones
Trypanosoma cruzi
Molecular docking
Trypanothione reductase
Old Yellow Enzyme

ABSTRACT

Herein, the design and synthesis of new 2-phenyl(pyridinyl)benzimidazolequinones and their 5-phenoxy derivatives as potential anti-*Trypanosoma cruzi* agents are described. The compounds were evaluated *in vitro* against the epimastigotes and trypomastigote forms of *Trypanosoma cruzi*. The replacing of a benzene moiety in the naphthoquinone system by an imidazole enhanced the trypanosomicidal activity against *Trypanosoma cruzi*. Three of the tested compounds (**11a-c**) showed potent trypanosomicidal activity and compound **11a**, with IC_{50} of 0.65 μM on the trypomastigote form of *T. cruzi*, proved to be 15 times more active than nifurtimox. Additionally, molecular docking studies indicate that the quinone derivatives **11a-c** could have a multitarget profile interacting preferentially with trypanothione reductase and Old Yellow Enzyme.

1. Introduction

Chagas disease (CD), also called American trypanosomiasis, is caused by the protozoan parasite *Trypanosoma cruzi* (*T. cruzi*). CD is endemic in Central and South America; however, due to international migration, it is also found in non-endemic countries such as in the United States, Europe and Australia [1]. Currently, about 11 million people worldwide are infected and more than 10.000 deaths are estimated to occur annually from this disease [2]. Two main drugs are used for the treatment of CD benznidazole and nifurtimox (Nfx), both exhibit limited efficacy and present severe side effects [3]. Accordingly, there is a need for developing more effective drugs for the treatment of this disease. The trypanosomicidal activity exhibited by many natural occurring naphthoquinones [4] has stimulated the discovery and development of novel naphthoquinoidal compounds as new agents useful in CD therapy [5]. Recent results suggest that 2-aryloxynaphthoquinones (**I**, Fig. 1) [6–8] could be a good starting point to identify new potential molecular leads for the development of more effective anti-chagasic agents. Taking into account that the synthesis of bioisosteres has been a strategy in the search for new compounds with improved biological activity [9,10], in this study, we replaced the benzene moiety of the naphthoquinone system by an imidazole. Furthermore, diverse biological activities displayed by benzimidazolequinone derivatives such as compound **II** (Fig. 1), inhibitor of purine nucleoside phosphorylase of protozoan *Toxoplasma gondii* [11], and compounds **III** and **IV** (Fig. 1), with cytotoxic activity against a variety of cancer cell lines [12,13] or potent inhibitory activity against NAD(P)H:quinone oxidoreductase 1 (NQO1) and indoleamine 2,3-dioxygenase (IDO) [14,15] have been described. In previous studies on this type of benzimidazole-4,7-diones, the presence of the quinone structure instead of the aromatic analog, the imidazole ring instead of a pirrol ring, or 2-aromatic ring substituted benzimidazole-4,7-diones instead of aromatic ring fused analogues, seems to be associated with an increase in its toxicity [13,16,17], which may be due to different ways of interaction with DNA [18] or different reductive potentials [17].

In addition, considering that the trypanosomicidal activity of 4,7-benzimidazolediones has not been described, we report herein the synthesis of new aryloxy heterocyclic quinone derivatives **V** (Fig. 1), to evaluate their trypanosomicidal activity.

Currently, computer-aided drug discovery methods have played a major role in the development of new bioactive compounds [19,20]. These strategies became essential to choose specific targets and design

* Corresponding authors at: Departamento de Química Orgánica, Facultad de Química y de Farmacia, Pontificia Universidad Católica de Chile, Santiago 6094411, Chile (R. A. Tapia). Departamento de Ciencias Químicas, Facultad de Ciencias Exactas, Universidad Andrés Bello, Viña del Mar 2531015, Chile (J. Soto-Delgado).
E-mail addresses: rtapia@uc.cl (R.A. Tapia), jorge.soto@unab.cl (J. Soto-Delgado).

https://doi.org/10.1016/j.bioorg.2021.104823
Received 28 September 2020; Received in revised form 11 January 2021; Accepted 8 March 2021
Available online 12 March 2021

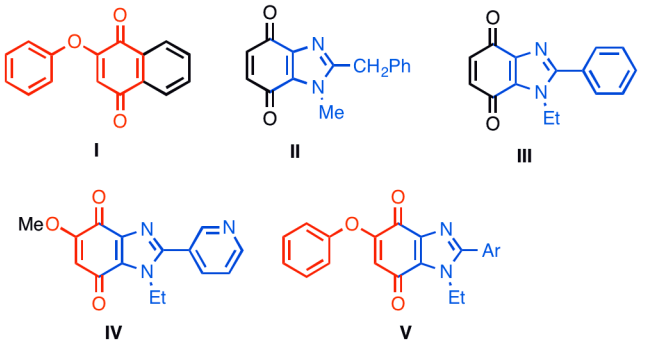

Fig. 1. Chemical structures of relevant biological active quinones (**I-IV**) and target phenoxy benzimidazolequinones (**V**).

new molecules as potential inhibitors. In order to understand the probable mechanism of action at the molecular level of the quinone derivatives, an induced-fit docking methodology was used with the purpose of identifying possible drug targets. Trypanothione reductase (*Tc*TR) and glyceraldehyde-3-phosphate dehydrogenase (*Tc*GAPDH) have been usual targets to explore the biological activities of naphthoquinones, and it was proposed that these compounds could act using a multi-target based mechanism [21,22]. However, in our recent studies a general relationship between trypanosomicidal of aryloxy-quinones and *Tc*TR enzyme inhibition could not be established [8]. Interestingly, recent studies indicated that *T. cruzi* Old Yellow Enzyme (*Tc*OYE), has a relevant role in the mechanism of action of benznidazole and Nfx, as well as some quinone derivatives [23–25]. Accordingly, induced-fit docking methodology was applied to investigate the probable binding mode to *Tc*OYE, and to shed light on the mechanisms of the trypanosomicidal effects of the new aryloxy-quinone derivatives **V**.

2. Results and discussion

2.1. Chemistry

Frequently, the synthesis of 2-arylbenzimidazoles involves condensation of *o*-phenylenediamines with aromatic aldehydes, but many of the reported methods require harsh reaction conditions and often a demanding work up [26]. After trying some milder methods, the best result was obtained using lanthanum chloride as catalyst [27]. The starting 1,4-dimethoxy-2,3-dinitrobenzene (**1**), was obtained following a literature method [28]. The reduction of **1** with tin granules and hydrochloric acid afforded 3,6-dimethoxybenzene-1,2-diamine (**2**) in excellent yield. The later was converted into benzimidazole derivatives **3a** (48%) and **3b** (85%) by condensation with the corresponding pyridine carboxaldehyde using lanthanum (III) chloride. Alkylation of benzimidazole derivatives **3a-b** by reaction with ethyl bromide in the presence of potassium carbonate and benzyltributylamonium chloride (BTBAC) gave the *N*-ethyl benzimidazole derivatives **4a-b** in excellent yields. Then, oxidation of the dimethoxy benzimidazole derivatives **4a-b** with silver (II) oxide and 6 N nitric acid provided benzimidazole-4,7-diones **5a** and **5b** in 67% and 58% yields, respectively (Scheme 1).

Next, in order to obtain bromobenzimidazole-4,7-dione **10b**, the reaction of **5a** with hydrobromic acid following a described methodology [29] was attempted but gave unsatisfactory results. Therefore, the synthesis of the target benzimidazole-4,7-diones was carried out as shown in Scheme 2. First, the selective reduction of 1,4-dimethoxy-2,3-dinitrobenzene (**1**) was achieved using hydrazine hydrate in the presence of the iron chloride and charcoal to give *o*-nitroaniline **6** in excellent yield. Then, *o*-nitroaniline **6** was treated with *N*-bromosuccinimide (NBS) in chloroform to afford compound **7** (70%, two steps) regioselectively. The one pot solvent-free iron-catalysed redox condensation [30] of *o*-nitroaniline **7** with benzylamine at 120 °C for 12 h afforded

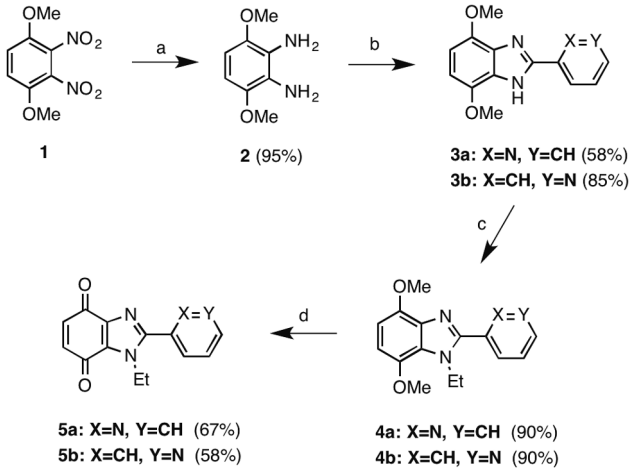

Scheme 1. *Reagents and conditions*: (a) Sn, HCl, reflux, 2 h; (b) $LaCl_3{\cdot}7H_2O$, ArCHO, MeCN, rt, 24 h; (c) i: DMF, K_2CO_3, BTBAC, 100 °C, 1 h; ii: EtBr rt 18 h; (d) THF, AgO, 6 N HNO_3, 5 min.

phenylbenzimidazole **8a** in a modest yield.

When the reaction was carried out under microwave irradiation at 140 °C for 15 min, phenylbenzimidazole **8a** was obtained in 85% yield. The same *o*-nitroaniline **7** was used for the synthesis of 2-pyridylbenzimidazoles applying Yang's method [31] with minor modifications. Thus, the reductive cyclization of *o*-nitroaniline **7** with the corresponding pyridinecarboxaldehyde in the presence of $Na_2S_2O_4$, yielded 2-pyridylbenzimidazoles **8b-d** in 65–78% yields.

Then, the alkylation of compounds **8a-d** with ethyl bromide, as above, gave the *N*-ethyl derivatives **9a-d** (62–74%). As a result of the tautomerism of the imidazole moiety, the alkylation of benzimidazoles **8** could occur at N-1 or N-3. It has been reported that the alkylation of 5-bromobenzimidazoles give the 1,5-isomer preferentially [32,33]. Here, only the 1,5-isomer was isolated, and their structures were established using ^1H, ^{13}C and 2D NMR techniques and further confirmed by single crystal X-ray analysis of two representative compounds, **9a** and **9b** (Fig. 2 and Table 1).

Oxidative demethylation of benzimidazoles **9a-d** with AgO/HNO_3, gave bromoquinones **10a-d** in good yields. Finally, phenoxybenzimidazole-4,9-diones **11a-d** were obtained in 50–58% yield by nucleophilic substitution reaction [34] of **10a-d** with phenol and potassium carbonate in dimethylformamide (Scheme 2).

2.2. Biological evaluation

The benzimidazole-4,7-dione derivatives (compounds **5**, **10** and **11**) were initially evaluated *in vitro* against the epimastigote form of *T. cruzi*, Dm28c strain. The convenience of this assay as a preliminary test to evaluate the *in vitro* trypanosomicidal activity has been recently described [35]. The compounds were evaluated at different concentrations (0.5–100 μM) to obtain a dose–response curve for calculation of IC_{50} values, including Nfx as reference drug. The IC_{50} values for all quinones on the epimastigote form of *T. cruzi* as well as the cytotoxicity using mammalian Vero cells and the selectivity index (SI = IC_{50} Vero cell/IC_{50} epimastigote form) are shown in Table 2. Interestingly, all compounds were more actives than Nfx on epimastigotes form *T. cruzi*. Comparing quinones **5a**, **5b** and **10a-d** with their corresponding phenoxybenzimidazole-4,7-diones **11a-d** (IC_{50} = 1.42–4.07 μM) an increase on the trypanosomicidal activity was observed. Only compounds **10b** and **11b** shown similar activity (Table 2).

Subsequently, the trypanosomicidal activity of benzimidazole-4,7-dione derivatives was assayed *in vitro* against the trypomastigote infective form of *T. cruzi* (Dm28c strain). Firstly, the viability of parasites was evaluated at a concentration of 5 μM. The phenoxyquinones **11** showed

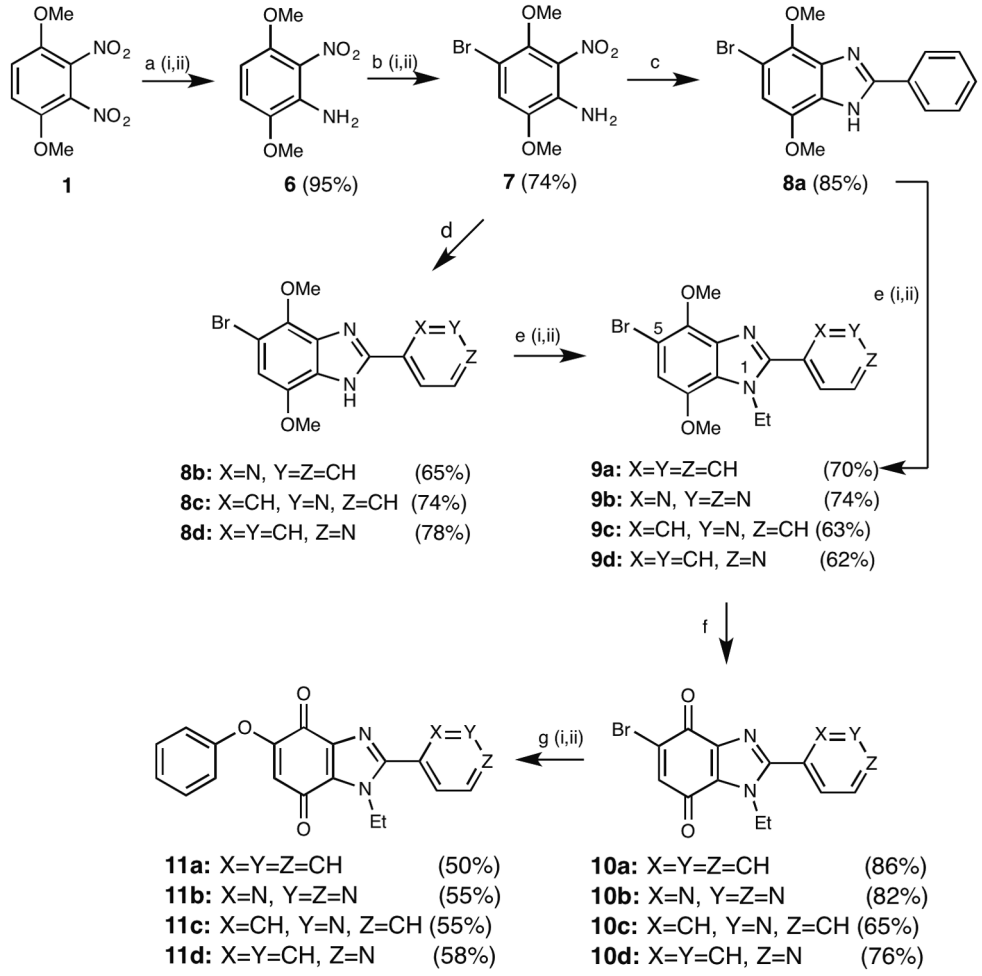

Scheme 2. *Reagents and conditions*: (a) i: Activated charcoal, $FeCl_3{\cdot}6H_2O$, MeOH, 65 °C, 1 h; ii: H_2NNH_2; (b) i: $CHCl_3$, NBS, −5 °C, 5 h; ii: rt, 20 h; (c) $PhCH_2NH_2$, $FeCl_3{\cdot}6H_2O$, 140 °C, 15 min; (d) 1 M $Na_2S_2O_4$, PyrCHO, EtOH, 70 °C, 10 h; (e) i: DMF, K_2CO_3, BTBAC, 100 °C, 1 h; ii: EtBr, rt, 18 h; (f) THF, AgO, 6 N HNO_3, 5 min; (g) i: PhOH, K_2CO_3, DMF, 25 °C, 1 h , ii: **10**, 25 °C, 12 h.

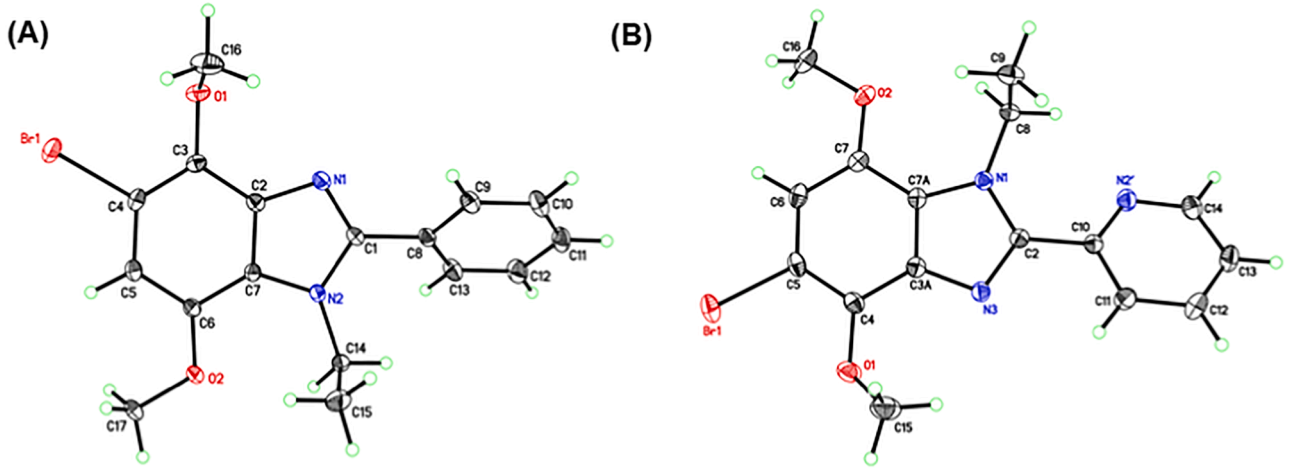

Fig. 2. Crystal structures of benzimidazoles **9a** (A) and **9b** (B).

significant inhibition against trypomastigote forms of *T. cruzi*, with viability percentages in the range of 13.1% to 24.1% versus 85% for Nfx. Then, quinones **11a-d** and **I** were evaluated at 0.1–5 μM concentrations to determine their IC_{50} values. Noteworthy, phenoxyquinones **11a-d** (IC_{50} = 0.65–1.39 μM) exhibited higher activity on the trypomastigote form of *T. cruzi* than on the epimastigote form of the parasite and compound **11a** proved to be 15 times more active than Nfx. It is important to highlight that the trypomastigote form is more relevant from the clinical perspective, because is the parasite infective form. Therefore, this result is very relevant within the study. Although the SI of compounds **11a-c** (SI = 10.6–11.5) are lower than Nfx (SI > 20), in agreement to some authors, potential antichagasic agents must have

Table 1
X-ray crystallographic data for compounds **9a** and **9b**.

Compound	9a	9b
Chemical formula	$C_{16}H_{14}BrCl_3N_2O_2$	$C_{16}H_{16}BrN_3O_2$
Formula weight	452.55	362.23
Crystal system, space group	Monoclinic, $P2_1/c$	Monoclinic, $P2_1/c$
Temperature (K)	120(2) K	120(2) K
Wavelength	0.71073 Å	0.71073 Å
Crystal system	monoclinic	monoclinic
Space group	$P2_1/c$	$P2_1/c$
Unit cell dimensions		
a, b, c (Å)	12.026(6), 15.567(6), 10.013(4)	10.2655(4),14.9077(6), 10.8243(4)
α, β, γ (°)	90, 111.494(4), 90	90, 116.4950(10), 90
Volume (Å^3)	1744.1(13)	1550.8(4)
Z, Calculated density	4, 1.723 g.cm^{-3}	4, 1.623 g.cm^{-3}
Radiation type	Mo Kα	Mo Kα
Absorption coefficient (μ)	2.828 mm^{-1}	2.784 mm^{-1}
F(000)	904	736
Crystal colour, habit	colourless, rod	colourless, block
Crystal size	0.246 × 0.053 × 0.052 mm^3	0.199 × 0.169 × 0.140 mm^3
θ range for data collection	1.820 to 26.752°	2.217 to 28.364°
Index ranges	$-15 \le h \le 15$, $-19 \le k \le 19$, $-12 \le l \le 12$	$-12 \le h \le 13$, $-19 \le k \le 19$, $-14 \le l \le 13$
Reflections collected	20,762	22,433
Independent reflections	3711 [R_{int} = 0.1381]	3703 [R_{int} = 0.0294]
Completeness to θ = 25.242°	99.9%	100.0%
Data Collection		
Absorption correction	Numerical	Numerical
Max. and min. transmission	0.9802, 0.6936	0.8142, 0.6917
Refinement method	Full-matrix least-squares on F^2	Full-matrix least-squares on F^2
Data / restraints / parameters	3711 / 0 / 220	3703 / 0 / 202
Goodness-of-fit on F^2	1.079	1.026
Final R indices [I > 2σ(I)]	R_1 = 0.0692, wR_2 = 0.1580	R_1 = 0.0253, wR_2 = 0.0550
R indices (all data)	R_1 = 0.1218, wR_2 = 0.1742	R_1 = 0.0356, wR_2 = 0.0582
Extinction coefficient	n/a	n/a
Largest diff. peak and hole	1.130, −1.063 e$^-$. Å^{-3}	0.432, −0.400 e$^-$.Å^{-3}

$IC_{50} \le 10$ μM and the SI (SI = IC_{50} Vero cells/IC_{50} trypomastigote forms) must be higher than 10 [36]. Three of the tested compounds (**11a-c**), meet both criteria and showed potent trypanosomicidal activity (Table 2). In this context, the phenoxyquinones described here for the first time can be considered as an important starting point for designing more active compounds with lower cytotoxicity against normal cells.

Considering the structural modification, it worth noting that those quinones having a fused imidazole system (**11a-d**) were most active than the reference compound 2-phenoxy-1,4-naphthoquinone (**I**). Regarding the C-2 substituent, the compounds showed the following order of decreasing trypanosomicidal activity **11a** (phenyl) > **11b** (2-pyridyl) > **11c** (3-pyridyl) > **11d** (4-pyridyl). Interestingly, similar results were described for the trypanosomicidal activity of 2-arylnaphthoimidazoles [37] and the antifungal activity of 6-arylamino-2-(pyridyl)-4,7-benzimidazolediones [38].

2.3. Molecular modelling studies

To investigate the potential targets of quinones derivatives and understand the mechanism of action at the molecular level, we next focused on target identification through induced-fit docking (IFD) methodology [39]. Glyceraldehyde-3-phosphate dehydrogenase (GAPDH) and trypanothione reductase (TR) has been common drugs targets to explore the trypanosomicidal activities of the naphthoquinones, proposing their multi-target biochemical pathway [21,40].

Recently, it has been described that the flavoprotein old yellow enzyme of *T. cruzi* (*Tc*OYE) is an oxidoreductase that has a relevant role in the mechanism of action of some trypanasomicidal naphthoquinones drugs [23]. The binding mode of β-lapachone, a trypanosomicidal agent, and other naphthoquinones was investigated by molecular docking and dynamics, suggesting that their binding to *Tc*OYE are stabilized predominantly through interactions with the isoalloxazine ring of flavin mononucleotide (FMN) prosthetic group and residues from the active-site pocket [24]. Therefore, in this study the phenoxybenzimidazole-4,9-diones and 2-phenoxy-1,4-naphthoquinone were used as ligands to perform molecular docking with *Tc*OYE as well as with *Tc*GAPDH and *Tc*TR for comparison purposes.

First, the IFD was carried out to study the interaction between *Tc*GAPDH and the new synthesized quinones. The *Tc*GAPDH (PDBCode: 1K3T), has a binding site characterized principally by the catalytic residue Cys166, together with Val255 and Asn335. These last two residues take importance due that probably are related to orientate correctly the side chain in order to receive the incoming NAD^+ cofactor [41]. In this work, the superimposed images in the docking simulation of the ligands is provided in supporting information (SI Figure S1) and best-ranked pose for the most active quinone **11a** at *Tc*GAPDH active site is shown in Fig. 3A. Compound **11a** shows H-bond interactions between oxygen atom of the quinone with NH fragment of Asn335 (2.1 Å), and nitrogen of Cys166 (2.4 Å), and hydrophobic interactions between phenyl rings with Arg249, Glu336, Arg12 and Ile13. This result is in accord to the proposed mechanism that Cys166-thiol may react with 2-phenoxy-1,4-naphthoquinones taking place a nucleophilic substitution reaction with the phenolate anion displacement and formation of a covalent C—S bond [6]. Nevertheless, the binding affinity to TcGAPDH predicted by IFD showed a low docking score respect to the other enzymes and there is no correlation with the trypanosomicidal activity of the compounds. (Table 3).

In relation with the interactions of naphthoquinones with *Tc*TR (PDBCode: 1BZL), it has been proposed the Z-site of this enzyme as binding site, which is characterized by a hydrophobic region defined by Phe396, Pro 462, and Leu399 [42,43]. Heterocyclic quinones **11a-d** and **I** showed good affinity to the Z-site of *Tc*TR, and the superimposed images in the docking simulation of the ligands is provided in supporting information (SI Figure S2). The most active compound **11a** showed the best affinity to *Tc*TR with a docking score of −7.905 kcal/mol (Table 3). For compound **11a** favourable H-bond interactions are suggested between carbonyl groups of the quinone system with Lys62 (2.5 Å) and Ser464 (2.2 Å), N-3 of imidazole scaffold also with Lys62 (2.1 Å) and the oxygen of the phenoxy group with Asn433 (2.4 Å). In addition, hydrophobic interactions between phenyl ring with the residues Leu63, Leu399 and Phe396 are proposed. It is important to point out that a similar binding mode was described previously for naphthoquinones, known by their non-competitive inhibition mechanism of *Tc*TR [8]. Probably, the key H-bond interaction between N-3 and Lys62 may be the reason that replacing phenyl group in **I** (IC_{50} = 2.09 μM) by imidazole scaffold led to the increase of trypanosomicidal activity of **11a** (IC_{50} = 0.63 μM). (Fig. 3B)

Next, the ligand-enzyme interactions of quinones with *Tc*OYE (PDBCode: 3ATZ) by IFD were investigated and the superimposed images of the ligands is provided in supporting information (SI Figure S3). The docking prediction showed a ternary complex *Tc*OYE/FMN/quinone with the FMN prosthetic group close enough to quinone **11a** that an electron/proton transfer could occur and stabilized by π-π stacking interactions between FMN and the ligand (Fig. 3**C**). Favourable H-bond interactions involving the carbonyl groups of the quinone system with Tyr364 (1.9 Å), Asn198 (2.1 Å) and His195 (3.0 Å) together with hydrophobic and π-π stacking interactions that present the

Table 2
In vitro activity, cytotoxicity and Selectivity Index (SI) of all quinones on epimastigote and trypomastigote forms of *T. cruzi* (Dm28c strain).

Compd.	Structure	IC_{50} [a] (μM) Epim.	Viability (%) Trypom. (5 μ_M)	IC_{50} [a] (μM) Trypom.	IC_{50} [a] (μM) Vero cell	Selectivity index	
						Epim.[b]	Trypom.[c]
5a	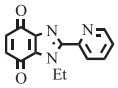	4.37 ± 0.45	33.89	n.d.	6.52 ± 0.79	1.5	n.d.
5b	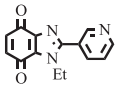	5.62 ± 0.50	38.19	n.d.	10.43 ± 1.86	1.9	n.d.
10a	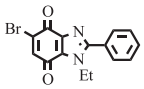	6.11 ± 0.52	46.74	n.d.	65.29 ± 2.81	10.7	n.d.
10b	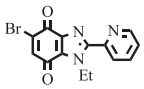	4.08 ± 0.32	61.22	n.d.	>100	>25	n.d.
10c	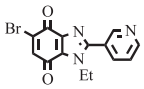	10.65 ± 0.80	66.10	n.d.	85.68 ± 1.29	8.1	n.d.
10d	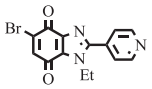	6.49 ± 0.60	61.13	n.d.	14.00 ± 0.76	2.2	n.d.
11a	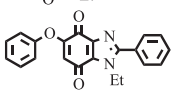	1.42 ± 0.07	15.98	0.65 ± 0.10	6.89 ± 0.50	4.9	10.6
11b	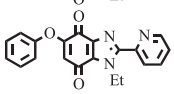	4.04 ± 0.30	19.04	0.88 ± 0.14	10.09 ± 0.70	2.5	11.5
11c	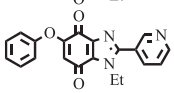	4.07 ± 0.27	13.05	0.96 ± 0.13	10.20 ± 0.79	2.5	10.6
11d	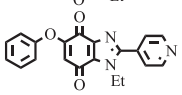	3.73 ± 0.32	24.12	1.39 ± 0.40	7.65 ± 0.66	2.1	5.5
I	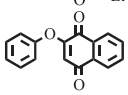	3.16 ± 0.28	35.17	2.09 ± 0.12	6.25 ± 0.65	2.1	3.0
	Nfx	21.05 ± 0.90	85.00	10.00 ± 0.40	>200	>9.5	>20

n.d.: not determined.
[a] Data are means of three independent experiments.
[b] Selectivity index: expressed as the ratio of IC_{50} in Vero cells to IC_{50} in epimastigotes.
[c] Selectivity index: expressed as the ratio of IC_{50} in Vero cells to IC_{50} in trypomastigotes.

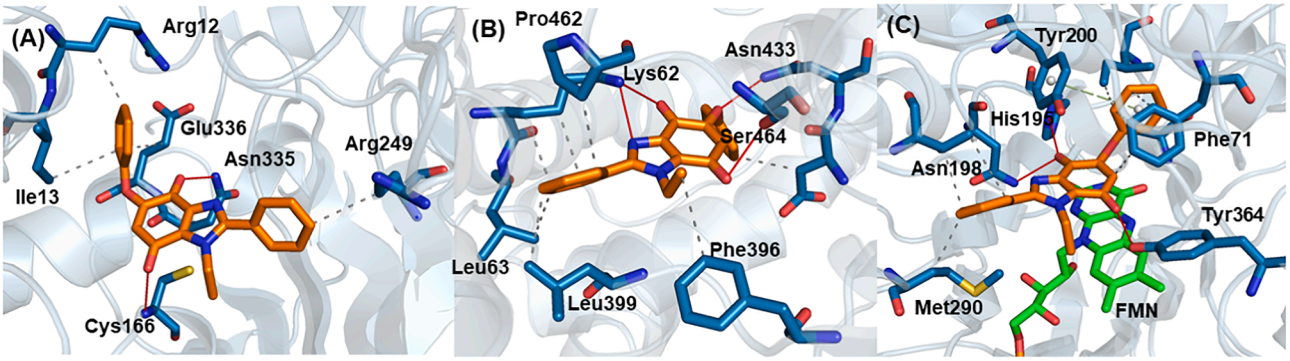

Fig. 3. Proposed binding mode for quinone **11a** at the active site of Glyceraldehyde-3-phosphate dehydrogenase (A), Trypanothione Reductase (B) and OLD Yellow Enzyme (C). (For interpretation of the references to colour in this figure legend, the reader is referred to the web version of this article.)

aromatic ring with residues Phe71 and Tyr200 are shown. This result suggested that *Tc*OYE could have an important role in the trypanosomicidal activity of quinones due to its reduction by the enzyme. Our study has shown that this contribution is performed at an average distance of 3.0 Å contributing with an important favourable interaction to produce hydride transfer from the reduced FMN to quinone substrates. It is worth noting that H-bond interactions with Tyr364, Asn198 and His195 are important for the ligand catalysis and were described for

Table 3
Binding affinity scores of quinones **11a-d** and **I** according to the Glide score (kcal/mol).

Compd.	*Tc*GAPDH	*Tc*TR	*Tc*OYE
5a	−5.46	−5.76	−6.77
5b	−5.00	−5.47	−6.17
10a	−5.00	−5.68	−6.76
10b	−4.93	−5.57	−7.52
10c	−5.05	−5.32	−6.17
10d	−6.01	−5.21	−6.61
11a	−5.55	−7.91	−9.40
11b	−6.19	−6.14	−7.68
11c	−6.06	−6.29	−7.62
11d	−6.17	−6.88	−8.06
I	−5.69	−6.95	−8.37

known inhibitors of *Tc*OYE [24].

In summary, these results suggest that the quinone derivatives could have a multitarget profile and might preferentially interact with *Tc*TR and *Tc*OYE which provides a molecular explanation of its anti-Trypanosoma activity. Therefore, we conclude that this strategy based on molecular docking over possible targets provides a helpful way for the rational design of more potent inhibitors and the future synthesis of highly potent trypanosomicidal compounds based on the phenoxyquinones derivatives.

3. Conclusions

In the search for new trypanosomicidal agents based on the replacing of the benzene moiety of the naphthoquinone system by imidazole led to phenoxy benzo[*d*]imidazole-4,7-diones as a promising class of multitarget compounds against *T. cruzi*. The analysis of the trypanosomicidal properties of these derivatives showed that phenoxyquinones **11a-d** were more active than the original naphthoquinone **I**, with IC_{50} values on the trypomastigote form of *T. cruzi* ranging from 0.65 to 1.39 μM. The most potent compound **11a** was nearly 15 times more active against the epimastigote form of the parasite (IC_{50} = 1.42 μM) and>15 times more active against the trypomastigote (IC_{50} of 0.65 μM), although with a much lower selectivity index against the tested Vero cells (SI = 10.6), than the Nfx as reference compound. These results stimulate further *in vivo* studies of these compounds and derivatives to definitely elucidate its multitarget profile. The results of induced fit molecular docking showed a better affinity of phenoxyquinones for *Tc*OYE and *Tc*TR, and that the imidazole scaffold has an important effect in the ligand-enzyme stabilization.

4. Experimental section

4.1. Chemistry

All chemicals were obtained from Merck or Sigma Aldrich and used without purification. Melting points (mp) were measured on an Electrothermal IA 9300 melting point apparatus and are uncorrected. ^{1}H and ^{13}C NMR spectra were recorded on a Bruker Advance 400 MHz spectrometer; chemical shifts (δ) are given in parts per million (ppm) and coupling constants (J) in Hertz (Hz). All assignments of NMR spectra were based on 2D NMR data (DEPT-135, COSY, HSQC and HMBC). High-resolution mass spectral analysis was carried out on a Bruker Impact II instrument. Infrared spectra (IR) were determined using an IRAffinity-1 Shimadzu spectrophotometer. The 1,4-dimethoxy-2,3-dinitrobenzene (**1**) starting material, was synthesized by nitration of 1,4-dimethoxybenzene according to the method described in literature [28].

4.1.1. Synthesis of 3,6-dimethoxybenzene-1,2-diamine (2)

To a stirred mixture of granular tin (15.1 g, 127.2 mmol) and 36% hydrochloric acid (60 mL) was added **1** (5.0 g, 21.9 mmol). The reaction mixture was heated to reflux for 2 h, and the resulting white solid was filtered. The solid was dissolved in water, the solution was made alkaline (pH = 8) with 5% ammonium hydroxide and extracted with chloroform (3x50 mL). The combined organic layers were dried over Na_2SO_4, filtered, and concentrated to give the crude product, which was purified by flash column chromatography (chloroform/hexane, 1:1) to give **2** (3.5 g, 95%); mp 86–87 °C (Lit. [28] 86–87 °C).

4.1.2. General procedure for preparing 4,7-dimethoxy-2-(pyridinyl)-1H-benzo[d]imidazoles (3a-b)

A mixture of 3,6-dimethoxybenzene-1,2-diamine (1.68 g, 10 mmol) (**2**), lanthanum (III) chloride heptahydrate (371.4 mg, 1.0 mmol) and the corresponding pyridine carboxaldehyde (10 mmol) in acetonitrile (60 mL) was stirred at room temperature for 24 h. After evaporation of the solvent, the residue was dissolved in ethyl acetate, washed with water, dried ($MgSO_4$) and concentrated. The crude products were purified by column chromatography (ethyl acetate/hexane, 1:1).

4.1.2.1. 4,7-Dimethoxy-2-(pyridin-2-yl)-1H-benzo[d]imidazole ***(3a).*** Colourless solid, mp 141–142 °C, yield 58%; IR (KBr, cm^{-1}) 3430, 1615, 1600, 1540, 1460, 1270, 1100; ^{1}H NMR (DMSO-d_6): 3.86 (s, 3H, OCH_3), 4.01 (s, 3H, OCH_3), 6.54 (d, J = 8.4 Hz, 1H), 6.60 (d, J = 8.4 Hz, 1H), 7.30 (dd, J = 1.2 and 4.9 Hz, 1H), 7.82 (dd, J = 1.2 and 7.8 Hz, 1H), 8.50–8.60 (m, 2H), 10.7 (s, 1H, NH); ^{13}C NMR (DMSO-d_6): 55.7 (2C), 121.5 (2C), 124.5 (2C), 136.8 (2C), 148.1 (2C), 148.9 (2C), 149.3(2C). HRMS (ESI$^+$): $[M+H]^+$ calcd. for $C_{14}H_{13}N_3O_2$, 256.1087; found, 256.1077.

4.1.2.2. 4,7-Dimethoxy-2-(pyridin-3-yl)-1H-benzo[d]imidazole ***(3b).*** Colourless solid, mp mp 218–220 °C (Lit. [44] 214–216 °C), yield 85%.

4.1.3. General procedure for synthesis of 1-ethyl-4,7-dimethoxy-2-(pyridinyl)-1H-benzo[d]imidazoles (4a-b)

To a solution of the corresponding 2-aryl-4,7-dimethoxy-*1H*-benzo[*d*]imidazole **3** (1.5 mmol) in DMF (2.0 mL) were added potassium carbonate (235 mg, 1.7 mmol) and benzyltributylamonium chloride (46.8 mg, 0.15 mmol) and the mixture was heated at 100 °C for 1 h. After cooling to room temperature, was added bromoethane (52.3 mg, 1.62 mmol) and the suspension was stirred for 18 h. The reaction mixture was concentrated under vacuum and the residue was purified by column chromatography (ethyl acetate/hexane, 1:2).

4.1.3.1. 1-Ethyl-4,7-dimethoxy-2-(pyridin-2-yl)-1H-benzo[d]imidazole ***(4a).*** Colourless solid, mp 100–101 °C, yield 90%; IR (KBr, cm^{-1}) 1600, 1530, 1480, 1440, 1270, 1210, 1120, 1090; ^{1}H NMR ($CDCl_3$): 1.40 (t, J = 6.5 Hz, 3H, CH_3) 3.85 (s, 3H, OCH_3), 3.94 (s, 3H, OCH_3), 5.00 (q, J = 6.5 Hz, 2H, CH_2) 6.5–6.60 (m, 2H), 7.20–7.25 (m, 1H), 7.70–7.75 (m, 1H), 8.35–8.40 (m, 1H), 8.55–8.60 (m, 1H); ^{13}C NMR ($CDCl_3$): 17.0, 42.3, 55.8 (2C), 101.3, 103.7, 123.4, 125.3, 127.1, 134.9, 136.4, 141.9, 146.1, 148.4, 148.9, 150.7. HRMS (ESI$^+$): $[M+H]^+$ calcd. for $C_{16}H_{17}N_3O_2$, 284.1400; found, 284.1388.

4.1.3.2. 1-Ethyl-4,7-dimethoxy-2-(pyridin-3-yl)-1H-benzo[d]imidazole ***(4b).*** Colourless solid, mp 115–117 °C, yield 90%; IR (KBr, cm^{-1}) 1635, 1527, 1473, 1430, 1378, 1270, 1108; ^{1}H NMR ($CDCl_3$): 1.36 (t, J = 7.3 Hz, 3H, CH_3) 3.87 (s, 3H, OCH_3), 3.92 (s, 3H, OCH_3), 4.38 (q, J = 7.3 Hz, 2H, CH_2) 6.52 (d, J = 8.5 Hz, 1H), 6.57 (d, J = 8.5 Hz, 1H), 7.35–7.40 (m, 1H), 8.02 (d, J = 7.8 Hz, 1H), 8.66 (d, J = 4.8 Hz, 1H), 8.91 (s, 1H); ^{13}C NMR ($CDCl_3$): 17.2, 41.5, 55.8 (2C), 101.8, 103.6, 123.3, 126.2, 135.3, 137.2, 136.4, 141.5, 146.0, 149.9, 150.4. HRMS (ESI$^+$): $[M+H]^+$ calcd. for $C_{16}H_{17}N_3O_2$, 284.1400; found, 284.1391.

4.1.4. General procedure for synthesis of 1-ethyl-2-pyridinyl-1H-benzo[d]imidazole-4,7-diones (5a-b)

To a stirred solution of appropriated 2-arilbenzimidazole **4** (0.2

mmol) in THF (2.5 mL), were added silver (II) oxide (70 mg; 0.6 mmol) and 6 N nitric acid (0.2 mL). After 5 min, the reaction mixture was diluted with water (5 mL) and extracted with chloroform (3x15 mL) The combined organic extracts were dried ($MgSO_4$), concentrated in vacuo, and the residue was purified by column chromatography (ethyl acetate/hexane, 1:2).

*4.1.4.1. 1-Ethyl-2-(pyridin-2-yl)-1H-benzo[d]imidazole-4,7-dione **(5a)**.* Yellow solid, mp 170–172 °C, yield 67%; IR (KBr, cm^{-1}) 1682, 1652, 1591, 1485, 1410, 1395; ^{1}H NMR ($CDCl_3$): 1.48 (t, $J = 7.0$ Hz, 3H, CH_3), 4.42 (q, $J = 7.0$ Hz, 2H, CH_2), 6.66 (d, $J = 10.3$ Hz, 1H), 6.72 (d, $J = 10.3$ Hz, 1H), 7.40–7.50 (m, 1H), 8.05 (d, $J = 7.6$ Hz, 1H), 8.76 (d, $J = 7.6$ Hz, 1H), 8.91 (s, 1H); ^{13}C NMR ($CDCl_3$): 17.0, 42.3, 55.8 (2C), 101.3, 103.7, 123.4, 125.3, 127.1, 134.9, 136.4, 141.9, 146.1, 148.4, 148.9, 150.7. HRMS (ESI^+): $[M+H]^+$ calcd. for $C_{14}H_{12}N_3O_2$, 254.0930; found, 254.0928.

*4.1.4.2. 1-Ethyl-2-(pyridin-3-yl)-1H-benzo[d]imidazole-4,7-dione **(5b)**.* Yield 58%, yellow solid mp 150–151 °C (Lit. [13]147–148 °C).

*4.1.5. Synthesis of 3,6-dimethoxy-2-nitroaniline **(6)***

A mixture of 1,4-dimethoxy-2,3-dinitrobenzene (4.56 g, 20 mmol) (**1**), activated charcoal (0.8 g), iron (III) chloride hexahydrate (324.4 mg, 1.2 mmol) in methanol (25 mL), was stirred at 65 °C for 1 h. Then, hydrazine monohydrate (3.84 mL, 79 mmol) was added drop wise and stirred at 65 °C for 1 h. The reaction was allowed to cool to room temperature and the solids were filtered and washed with methanol. The filtrate was dried ($MgSO_4$), concentrated and the residue was purified by column chromatography (ethyl acetate/hexane, 1:1) to give **6** as an orange solid (3.76 g, 95%), mp 68–69 °C (lit. [28] 67–68 °C).

*4.1.6. Synthesis of 4-bromo-3,6-dimetoxy-2-nitroaniline **(7)***

A solution of **6** (260 mg; 1.31 mmol) in chloroform (5 mL) was cooled to −5 °C, and a solution of *N*-bromosuccinimide (230 mg, 1.31 mmol) in acetonitrile (2 mL) was added dropwise. The mixture was stirred at −5 °C for 5 h, and then was further stirred for 20 h at room temperature. After evaporation of the solvents, the residue was purified by column chromatography (chloroform/hexane, 1:4) to afford **7** as an orange solid (255 mg, 74%), mp 131–132 °C; IR (cm^{-1}) 3510, 3390,1617, 1595, 1523, 1344; ^{1}H NMR ($CDCl_3$): 3.84 (s, 3H, OCH_3), 3.89 (s, 3H, OCH_3), 5.34 (s, 2H, NH_2), 6.90 (s, 1H); ^{13}C NMR ($CDCl_3$): 56.6, 62.7, 102.5, 115.3, 116.3, 134.5, 144.2. 145.3; HRMS (ESI^+): $[M + Na]^+$ calcd for $C_8H_9N_2NaO_4$, 298.9643; found, 298.9634.

*4.1.7. Synthesis of 5-bromo-4,7-dimethoxy-2-phenyl-1H-benzo[d] imidazole **(8a)***

A mixture of **7** (138.6 mg, 0.5 mmol), benzylamine (251 mg, 1.5 mmol), and iron (III) chloride hexahydrate (6.8 mg, 0.025 mmol) in a 10-mL pressure tube was stirred at 140 °C for 15 min using an Anton Paar Monowave 300 Microwave Synthesis Reactor (Anton Paar GmbH, Graz, Austria). After cooling, the reaction mixture was diluted with ethyl acetate, then filtered over a pad of Celite, and washed with ethyl acetate. The filtrates were dried ($MgSO_4$), evaporated and the residue was purified by flash chromatography on silica gel (ethyl acetate/hexane, 1:1) to afford compound **8a** (141.6 mg, 85%) as a colourless solid, mp 157–159 °C; IR (KBr, cm^{-1}) 3500, 3430, 1614, 1514, 1486, 1457, 1386, 1300; ^{1}H NMR (DMSO-d_6): 3.88 (s, 3H, OCH_3), 4.00 (s, 3H, OCH_3), 6.84 (s, 1H), 7.44–7.49 (m, 3H), 7.60–7.70 (m, 2H), 13.47 (s, 1H, NH); ^{13}C NMR (DMSO-d_6): 56.5, 61.1, 105.2, 107.8, 124.3 (2C), 126.1 (2C), 126.9, 134.5, 137.7, 142.3, 148.3, 148.9, 150.9; HRMS (ESI^+): $[M+H]^+$ calcd for $C_{15}H_{14}BrN_2O_2$, 333.0239; found, 333.0227.

*4.1.8. General procedure for synthesis of 5-bromo-4,7-dimethoxy-2-(pyridinyl)-1H-benzo[d]imidazoles **(8b-d)***

Freshly prepared 1 M aqueous sodium dithionite (261.2 mg, 1.5 mmol) was added to a stirred mixture of 4-bromo-3,6-dimetoxy-2-nitroaniline **7** (138.6 mg, 0.5 mmol) and the corresponding pyridine carboxaldehyde (0.5 mmol) in ethanol (2 mL), and the reaction mixture was heated at 70 °C for 10 h. After cooling, he resulting mixture was made alkaline with ammonium hydroxide and then extracted with ethyl acetate (3x10 mL). The combined organic layers were dried ($MgSO_4$) and the solvent was removed under vacuum. The crude product was purified by column chromatography on silica gel (ethyl acetate/hexane, 1:1).

*4.1.8.1. 5-Bromo-4,7-dimethoxy-2-(pyridin-2-yl)-1H-benzo[d]imidazole **(8b)**.* Colourless solid, mp 141–142 °C, yield 65%; IR (KBr, cm^{-1}) 3490, 3150, 1600, 1514, 1457, 1429, 1386, 1286; ^{1}H NMR (DMSO-d_6): 3.81 (s, 3H, OCH_3), 4.05 (s, 3H, OCH_3), 6.77 (s, 1H), 7.40 (dd, 1H, $J = 4.7$ and 7.9 Hz), 7.87 (t, 1H, $J = 7.9$ Hz), 8.21 (d, 1H, $J = 7.9$ Hz), 8.61 (d, 1H, $J = 4.7$ Hz), 13.40 (s, 1H, NH). ^{13}C NMR (DMSO-d_6): 56.6, 61.4, 122.4, 125.2, 137.9 (4C), 148.7 (2C), 149.8 (2C), 150.9 (2C); HRMS (ESI^+): $[M+H]^+$ calcd. for $C_{14}H_{13}BrN_3O_2$, 334.0191; found, 334.0181.

*4.1.8.2. 5-Bromo-4,7-dimethoxy-2-(pyridin-3-yl)-1H-benzo[d]imidazole **(8c)**.* Yellow solid, mp 240–242 °C, yield 74%; IR (KBr, cm^{-1}) 3450, 1604, 1507, 1475, 1453, 1416, 1386, 1280, ^{1}H NMR (DMSO-d_6): 3.91 (s, 3H, OCH_3), 4.14 (s, 3H, OCH_3), 6.88 (s, 1H), 7.49–7.54 (m, 1H), 8.52 (d, $J = 7.5$ Hz, 1H), 8.62 (d, $J = 4.0$ Hz, 1H), 9.36 (s, 1H), 13.42 (s, 1H, NH); ^{13}C NMR (DMSO-d_6): 56.7, 61.3, 105.4, 108.1, 124.5, 126.3 (2C), 127.2, 134.8, 137.9, 142.5, 148.5, 149.1, 151.2; HRMS (ESI^+): $[M+H]^+$ calcd. for $C_{14}H_{13}BrN_3O_2$, 334.0191; found, 334.0183.

*4.1.8.3. 5-Bromo-4,7-dimethoxy-2-(pyridin-4-yl)-1H-benzo[d]imidazole **(8d)**.* Yellow solid, mp 190–192 °C, yield 78%; IR (KBr, cm^{-1}) 3450, 3260, 1600, 1510, 1450, 1390, 1275; ^{1}H NMR (DMSO-d_6): 3.86 (s, 3H, OCH_3), 4.01 (s, 3H, OCH_3), 6.82 (s, 1H), 8.08 (d, $J = 5.0$ Hz, 2H), 8.64 (d, $J = 5.0$ Hz, 2H), 13.47 (s, 1H, NH); ^{13}C NMR (DMSO-d_6): 56.5, 61.3, 108.0, 121.1, 137.1 (4C), 148.8 (4C), 150.8 (2C); HRMS (ESI^+): $[M+H]^+$ calcd. for $C_{14}H_{13}BrN_3O_2$, 334.0191; found, 334.0182.

*4.1.9. Synthesis of 2-(aryl)-5-bromo-1-ethyl-4,7-dimethoxy-1H-benzo[d] imidazoles **(9a-d)***

The general procedure described for the preparation of **4a-b** (*2.1.3.*) from **3a-b** was utilized to synthesize compounds **9a** from **8a** and **9b-d** from **8b-d**.

*4.1.9.1. 5-Bromo-1-ethyl-4,7-dimethoxy-2-phenyl-1H-benzo[d]imidazole **(9a)**.* White solid, mp 157–158 °C, yield 70%; IR (KBr, cm^{-1}) 1610, 1510, 1475, 1460, 1410, 1290, 1240, 1140, 1085; ^{1}H NMR ($CDCl_3$): 1.37 (t, $J = 7.0$ Hz, 3H, CH_3), 3.92 (s, 3H, OCH_3), 4.21 (s, 3H, OCH_3), 4.36 (q, $J = 7.0$ Hz, 2H, CH_2), 6.81 (s, 1H), 7.48–7.51 (m, 3H), 7.65–7.69 (m, 2H). ^{13}C NMR ($CDCl_3$): 17.2, 41.5, 56.1, 61.5, 106.3, 107.6, 125.9 (2C), 128.7 (2C), 129.6, 129.8, 130.3, 137.9, 142.8, 142.9, 153.5 ppm. HRMS (ESI^+): $[M+H]^+$ calcd. for $C_{17}H_{18}BrN_2O_2$, 361.0552; found, 361.0549.

*4.1.9.2. 5-Bromo-1-ethyl-4,7-dimethoxy-2-(pyridin-2-yl)-1H-benzo[d] imidazole **(9b)**.* White solid, mp 114–115 °C, yield 74%; IR (KBr, cm^{-1}) 1625, 1590, 1500, 1430, 1390, 1290, 1125; ^{1}H NMR ($CDCl_3$): 1.44 (t, $J = 7.0$ Hz, 3H, CH_3), 3.93 (s, 3H, OCH_3), 4.25 (s, 3H, OCH_3), 4.50 (q, $J = 7.0$ Hz, 2H, CH_2), 6.80 (s, 1H), 7.30–7.35 (m, 1H), 7.81 (t, $J = 7.8$ Hz, 1H), 8.34 (d, $J = 7.8$ Hz, 1H), 8.67 (d, $J = 5.0$ Hz, 1H); ^{13}C NMR ($CDCl_3$): 17.0, 42.3, 56.2, 61.5, 105.9, 108.0, 123.8, 125.3, 126.9, 136.7, 137.5, 142.8, 143.3, 148.7, 149.6, 150.4; HRMS (ESI^+): HRMS (ESI^+): $[M+H]^+$ calcd. for $C_{16}H_{17}BrN_3O_2$, 362.0504; found, 362.0505.

*4.1.9.3. 5-Bromo-1-ethyl-4,7-dimethoxy-2-(pyridin-3-yl)-1H-benzo[d] imidazole **(9c)**.* White solid, mp 78–80 °C, yield 63%; IR (KBr, cm^{-1}) 1615, 1520, 1470, 1440, 1390, 1290; ^{1}H NMR ($CDCl_3$): 1.39 (t, $J = 7.0$ Hz, 3H, CH_3), 3.92 (s, 3H, OCH_3), 4.18 (s, 3H, OCH_3), 4.37 (q, $J = 7.0$

Hz, 2H, CH_2), 6.81 (s, 1H), 7.42–7.47 (m, 1H), 8.04 (t, $J = 5.0$ Hz, 1H), 8.73 (d, $J = 5.0$ Hz, 1H), 8.92 (s, 1H); ^{13}C NMR ($CDCl_3$): 17.3, 41.8, 56.2, 61.6, 106.7, 108.1, 123.6, 126.1, 126.7, 137.3, 138.1, 142.9, 143.0, 149.9, 150.3, 150.8; HRMS (ESI^+): $[M+H]^+$ calcd. for $C_{16}H_{17}BrN_3O_2$, 362.0504; found, 362.0495.

*4.1.9.4. 5-Bromo-1-ethyl-4,7-dimethoxy-2-(pyridin-4-yl)-1H-benzo[d] imidazole (**9d**).* White solid, mp 160–161 °C, yield 62%; IR (KBr, cm^{-1}) 1615, 1510, 1455, 1420, 1385, 1295, 1120; ^1H NMR ($CDCl_3$): 1.40 (t, $J = 7.0$ Hz, 3H, CH_3), 3.92 (s, 3H, OCH_3), 4.18 (s, 3H, OCH_3), 4.40 (q, $J = 7.0$ Hz, 2H, CH_2), 6.81 (s, 1H), 7.61 (d, $J = 5.0$ Hz, 2H), 8.76 (d, $J = 5.0$ Hz, 2H), ^{13}C NMR ($CDCl_3$): 17.2, 41.7, 56.2, 61.5, 106.7, 108.3, 123.7 (2C), 126.2 (4C). 137.9, 142.9, 150.3 (2C). HRMS (ESI^+): $[M+H]^+$ calcd. for $C_{16}H_{17}BrN_3O_2$, 362.0504; found, 362.0496.

*4.1.10. Synthesis of 2-aryl-5-bromo-1-ethyl-1H-benzo[d]imidazole-4,7-diones (**10a-d**)*

The general procedure described for the preparation of ***5a-b*** from **4a-b** (*2.1.4.*) was utilized to synthesize compounds ***10a-d*** from **9a-d**.

*4.1.10.1. 5-Bromo-1-ethyl-2-phenyl-1H-benzo[d]imidazole-4,7-dione (**10a.**).* Orange solid, mp 178–179.5 °C, yield 86%; IR (KBr, cm^{-1}) 1695, 1650, 1590, 1480, 1430, 1380, 1225, 1190; ^1H NMR ($CDCl_3$): 1.49 (t, $J = 7.1$ Hz, 3H, CH_3), 4.44 (q, $J = 7.1$ Hz, 2H, CH_2), 7.22 (s, 1H), 7.55–7.75 (m, 5H); ^{13}C NMR ($CDCl_3$): 16.4, 42.2, 128.4 (2C), 129.3 (2C), 129.6 (2C), 131.1, 131.4, 137.8, 138.4, 154.6, 173.5, 175.8; HRMS (ESI^+): $[M+H]^+$ calcd. for $C_{15}H_{12}BrN_2O_2$, 332.0060; found, 332.0038.

*4.1.10.2. 5-Bromo-1-ethyl-2-(pyridin-2-yl)-1H-benzo[d]imidazol-4,7-dione (**10b**).* Orange solid, mp 175–177 °C, yield 82%; IR (KBr, cm^{-1}) 1690, 1660, 1580, 1530, 1470, 1420, 1380, 1270; ^1H NMR ($CDCl_3$): 1.55 (t, $J = 6.9$ Hz, 3H, CH_3), 5.12 (q, $J = 6.9$ Hz, 2H, CH_2), 7.33 (s, 1H), 7.45 (t, $J = 7.7$ Hz, 1H), 7.91 (t, $J = 7.7$ Hz, 1H), 8.44 (d, $J = 7.7$ Hz, 1H), 8.74 (d, $J = 7.7$ Hz, 1H); ^{13}C NMR ($CDCl_3$): 16.4, 43.6, 125.0, 125.8, 132.2, 137.5, 138.4, 138.4, 141.0, 149.1, 150.8, 149.3, 173.7, 176.0; HRMS (ESI^+): $[M+H]^+$ calcd for $C_{14}H_{11}BrN_3O_2$, 332.0035; found, 332.0034.

*4.1.10.3. 5-Bromo-1-ethyl-2-(pyridin-3-yl)-1H-benzo[d]imidazol-4,7-dione (**10c**).* Orange solid, mp 174–176 °C, yield 65%; IR (KBr, cm^{-1}) 1690, 1660, 1580, 1540, 1470, 1405, 1295; ^1H NMR ($CDCl_3$): 1.50 (t, $J = 7.1$ Hz, 3H, CH_3), 4.44 (q, $J = 7.1$ Hz, 2H, CH_2), 7.22 (s, 1H), 7,52 (t, $J = 7.7$ Hz, 1H), 8.07 (d, $J = 7.7$ Hz, 1H), 8.87 (d, $J = 7.7$ Hz, 2H); RMN ^{13}C (100 MHz; $CDCl_3$): 16.5, 42.4, 124.2, 124.9, 131.7, 137.4, 137.9, 138.5, 141.5, 149.6, 151.5, 151.9, 173.3, 175.7; HRMS (ESI^+): $[M+H]^+$ calcd for $C_{14}H_{11}BrN_3O_2$, 332.0035; found, 332.0034.

*4.1.10.4. 5-Bromo-1-ethyl-2-(pyridin-4-yl)-1H-benzo[d]imidazol-4,7-dione (**10d**).* Yellow solid, mp 185–186 °C, yield 76%; IR (KBr, cm^{-1}): 1700, 1650, 1595, 1570, 1530, 1490, 1430, 1420, 1280; ^1H NMR ($CDCl_3$): 1.49 (t, $J = 7.0$ Hz, 3H, CH_3), 4.45 (q, $J = 7.0$ Hz, 2H, CH_2), 7.21 (s, 1H), 7.60 (d, $J = 4.3$ Hz, 2H), 8.81 (d, $J = 4.3$ Hz, 2H) ppm; RMN ^{13}C (100 MHz; $CDCl_3$):16.2, 42.2, 123.3 (2C), 131.6, 135.9, 137.7, 138.5, 141.2 (2C), 150.7, 173.0, 175.5; HRMS (ESI^+): $[M+H]^+$ calcd for $C_{14}H_{11}BrN_3O_2$, 332.0035; found, 332.0040.

*4.1.11. General procedure for preparing 2-aryl-1-ethyl-5-phenoxy-1H-benzo[d]imidazole-4,7-diones (**11a-d**)*

A mixture of phenol (9.41 mg, 0.1 mmol) and K_2CO_3 (41.5 mg, 0.3 mmol) in DMF (0.5 mL) was stirred for 1 h at 25 °C. Then, the corresponding bromoquinone **10** (0.1 mmol) was added and the reaction mixture was stirred at 25 °C for 12 h. The reaction mixture was diluted with water (5 mL) and extracted with chloroform (3x15 mL). The combined organic extracts were dried ($MgSO_4$), concentrated in vacuo, and the residue was purified by column chromatography (ethyl acetate/hexane, 1:2).

*4.1.11.1. 1-Ethyl-5-phenoxy-2-phenyl-1H-benzo[d]imidazole-4,7-dione (**11a**).* Orange solid, mp 190–192 °C, yield 50%; IR (KBr, cm^{-1}) 1710, 1660, 1615, 1600, 1540, 1430, 1380, 1320, 1200; ^1H NMR ($CDCl_3$): 1.43 (t, $J = 7.0$ Hz, 3H, CH_3); 4.40 (q, $J = 7.0$ Hz, 2H, CH_2); 5.58 (s, 1H); 7.14 (d, $J = 7.4$ Hz, 2H); 7.31 (t, $J = 7.4$ Hz, 1H); 7.46 (t, $J = 7.4$ Hz, 2H); 7.43–7.70 (m, 5H); ^{13}C NMR ($CDCl_3$): 16.2, 41.8, 110.4 (2C), 121.2, 126.7, 128.6 (2C). 129.0 (4C), 129.4 (2C), 130.5, 130.6, 140.6, 153.2, 160.1, 175.2, 178.5. HRMS-ESI: $[M+H]^+$ calcd for $C_{21}H_{17}N_2O_3$, 345.1239; found, 345.1237.

*4.1.11.2. 1-Ethyl-5-phenoxy-2-(pyridin-2-yl)-1H-benzo[d]imidazol-4,7-dione (**11b**).* Red solid, mp 177–178 °C, yield 55%; IR (KBr, cm^{-1}) 1710, 1650, 1610, 1595, 1535, 1480, 1420, 1390, 1205; ^1H NMR ($CDCl_3$): 1.45 (t, $J = 6.9$ Hz, 3H, CH_3), 5.04 (q, $J = 6.9$ Hz, 2H, CH_2), 5.57 (s, 1H), 7.10–7.38 (m, 4H), 7.44 (t, $J = 7.8$ Hz, 2H), 7.83 (t, $J = 7.8$ Hz, 1H), 8.38 (d, $J = 7.2$ Hz, 1H), 8.65 (d, $J = 4.3$ Hz, 1H); ^{13}C NMR ($CDCl_3$): 16.4, 43.4, 111.2 (2C), 121.5 (C), 124.8, 125.6, 126.9, 130.8 (2C), 132.5, 137.4, 140.4, 149.2, 149.4, 150.6, 153.5, 160.3, 175.6, 178.7; HRMS-ESI: $[M+H]^+$ calcd for $C_{20}H_{16}N_3O_3$, 346.1192; found, 346.1187.

*4.1.11.3. 1-Ethyl-5-phenoxy-2-(pyridin-3-yl)-1H-benzo[d]imidazol-4,7-dione (**11c**).* Yellow solid, mp 158–159 °C, yield 55%; IR (KBr, cm^{-1}): 1700, 1660, 1612, 1580, 1520, 1495, 1400, 1390, 1330, 1225, 1195; ^1H NMR ($CDCl_3$): 1.46 (t, $J = 7.1$ Hz, 3H, CH_3), 4.41 (q, $J = 7.1$ Hz, 2H, CH_2), 5.60 (s, 1H), 7.13 (d, $J = 7.4$ Hz, 2H), 7.31 (t, $J = 7.4$ Hz, 1H), 7.43–7.49 (m, 3H), 8.07 (d, $J = 7.4$ Hz, 1H), 8.78 (d, $J = 7.4$ Hz, 1H), 8.93 (s, 1H); ^{13}C NMR ($CDCl_3$): 17.2, 42.9, 111.3 (2C), 122.0, 124.7, 125.9, 127.6, 131.4, 132.6, 138.1, 141.6, 150.3, 151.9, 152.4, 153.9, 161.0, 175.9, 179.1; HRMS-ESI: $[M+H]^+$ calcd for $C_{20}H_{16}N_3O_3$, 346.1192; found, 346.1188.

*4.1.11.4. 1-Ethyl-5-phenoxy-2-(pyridin-4-yl)-1H-benzo[d]imidazole-4,7-dione (**11d**).* Yellow solid, mp 176–177 °C, yield 58%; IR (KBr, cm^{-1}) 1645, 1615, 1390, 1355, 1310, 1200; ^1H NMR ($CDCl_3$): 1.48 (t, $J = 6.8$ Hz, 3H, CH_3), 4.45 (q, $J = 6.8$ Hz, 2H, CH_2), 5.61 (s, 1H), 7.09–7.34 (m, 3H), 7.46 (t, $J = 7.3$ Hz, 2H), 7.63 (d, $J = 4.0$ Hz, 2H), 8.82 (d, $J = 4.0$, 2H); ^{13}C NMR ($CDCl_3$): 16.6, 42.4, 151.2 (2C), 141.0, 136.5, 132.3, 130.9 (2C), 127.1, 123.6 (2C), 121.5, 110.9 (2C); HRMS-ESI: $[M+H]^+$ calcd for $C_{20}H_{16}N_3O_3$, 346.1192; found, 346.1188.

4.2. Crystal structure determination

X-ray data for **9a** and **9b** were collected on a Bruker AXS APEX3 diffractometer using a combination of ω- and φ-scans of 0.5°. Data were corrected for absorption and polarization effects and analyzed for space group determination [45]. The structures were solved by dual-space methods and expanded routinely [46]. The models were refined by full-matrix least-squares analysis of F^2 against all reflections [47]. All non-hydrogen atoms were refined with anisotropic atomic displacement parameters. Unless otherwise noted, hydrogen atoms were included in calculated positions. Atomic displacement parameters for the hydrogens were tied to the equivalent isotropic displacement parameter of the atom to which they are bonded ($U_{iso}(H) = 1.5U_{eq}(C)$ for methyl, $1.2U_{eq}(C)$ for all others). The crystal data, data collection and structure refinement details of compounds **9a** and **9b** are tabulated in Table 1.

4.3. Biological evaluation

4.3.1. In vitro anti-T. Cruzi activity on epimastigotes.

T. cruzi epimastigotes, Dm28c strain, were grown at 28 °C in Diamond's monophasic medium supplemented with 4 μM hemin and 5% (v/v) foetal bovine serum as described earlier [48]. The compounds were tested at a starting concentration of 0.5–100 μM and were added to

suspensions of $3{\cdot}10^6$ parasites/mL and incubated at 28 °C for 24 h. After this period, trypanosomicidal activity was measured using MTT [3–(4,5-dimethylthiazol-2-yl)-2,5-diphenyltetrazolium bromide] assay [49]. MTT was added to a final concentration of 0.5 mg/mL with phenazine methosulfate (0.22 mg/mL) and incubated at 37 °C for 4 h. The parasites were solubilized in 10% sodium dodecyl sulfate-0.01 M HCl and incubated overnight. Formazan crystal formation was measured at 570 nm using an ELISA spectrophotometer (Labsystems Multiskan MS, Finlandia). A full dose–response curve was constructed for all compounds to determine the concentration inhibiting 50% of parasite growth (IC_{50} value). The IC_{50} values were obtained using non-linear dose response curve-fitting analysis (log of concentration vs percentage of viable cells) via Graph Pad Prism 5 software. Reported values are means of at least three independent experiments.

4.3.2. *In vitro anti-T. Cruzi activity on trypomastigotes.*

VERO cells infected with Dm28c trypomastigotes, as described previously [48], were suspended in RPMI supplemented with foetal bovine serum 5% and penicillin–streptomycin at a final density of $1x10^7$ parasites/mL. Then, viability assays at different concentrations of the compounds (0.1–10 μM) were determined using MTT method and IC_{50} values were obtained as above.

4.3.3. *Cytotoxicity assay*

Vero cells were supported ($1x10^5$ cells/well) in RPMI 1640 medium supplemented with 10% foetal bovine serum, penicillin (100 μg/ml)/streptomycin (100 μg/mL) and sodium bicarbonate (0.22%), at 37 °C, in humidified air with 5% CO_2. Then, cells were exposed to compounds (0.5–100 μM) under study for 48 h and cell viability was determined using MTT method.

4.4. *Molecular modelling studies*

The crystal structures of the proteins TcTR (PDBCode: 1BZL) [50], TcGAPDH (PDBCode: 1K3T) [51] and TcOYe (PDBCode: 3ATZ) [52] were downloaded from the Protein Data Bank (PDF). The initial setup of selected proteins for calculations was prepared using Schrödinger's Protein Preparation Wizard [53] to add hydrogens, assign bond orders, and generate rotamers and protonation states. All compounds were prepared using the Ligand Preparation software [54], while ionization/tautomeric states were predicted using Epik program [55]. The docking calculations using rigid-receptor and flexible-ligand were performed with Glide through the Extra Precision (XP) mode [56]. Rigid XP (extra precision) and induced fit docking was performed using the Glide package from Schrödinger. Rigid dockings were performed using extra precision (XP), ligand sampling was set to flexible, and the planarity of conjugated pi groups was enhanced. For conformer generation, an energy window of 3.5 kcal/mol was used, and the enhanced sampling option was selected. For induced fit docking, the standard protocol with default settings was employed. After molecular docking, all protein–ligand complexes, were prepared by the PLIP software [57] in the PDB format and directly visualized in the PyMOL Molecular Graphics System [58].

Declaration of Competing Interest

The authors declare that they have no known competing financial interests or personal relationships that could have appeared to influence the work reported in this paper.

Acknowledgements

This work was supported by FONDECYT-CHILE Grant 11150988 and 1150307. J.S-D wishes to thank to Dr. Danilo Gonzalez and The Center for Bioinformatics and Integrative Biology (CBIB) UNAB for computational support and providing licenses to use the corresponding software packages. C.L.L. thanks CONICYT for a doctoral fellowship.

Appendix A. Supplementary data

Supplementary data to this article can be found online at https://doi.org/10.1016/j.bioorg.2021.104823.

References

[1] J.R. Coura, P.A. Vinas, Chagas disease: a new worldwide challenge, Nature 465 (2010) S6–S7.
[2] K.M. Bonney, Chagas disease in the 21st century: a public health success or an emerging threat? Parasite 21 (2014) 11.
[3] J.A. Castro, M.M. de Mecca, L.C. Bartel, Toxic side effects of drugs used to treat Chagas disease (American trypanosomiasis), Hum. Exp. Toxicol. 25 (2006) 471–479.
[4] A.V. Pinto, S.L. de Castro, The trypanocidal activity of naphthoquinones: A review, Molecules 14 (2009) 4570–4590.
[5] C.O. Salas, M. Faúndez, A. Morello, J.D. Maya, R.A. Tapia, Natural and synthetic naphthoquinones active against trypanosoma cruzi: An initial step towards new drugs for Chagas disease, Curr. Med. Chem. 18 (2011) 144–161.
[6] F. Prati, C. Bergamini, M.T. Molina, F. Falchi, A. Cavalli, M. Kaiser, R. Brun, R. Fato, M.L. Bolognesi, 2-Phenoxy-1,4-naphthoquinones: From a multitarget antitrypanosomal to a potential antitumor profile, J. Med. Chem. 58 (2015) 6422–6434.
[7] K. Vázquez, C. Espinosa-Bustos, J. Soto-Delgado, R.A. Tapia, J. Varela, E. Birriel, R. Segura, J. Pizarro, H. Cerecetto, M. González, M. Paulino, C.O. Salas, New aryloxy-quinone derivatives as potential anti-Chagasic agents: Synthesis, trypanosomicidal activity, electrochemical properties, pharmacophore elucidation and 3D-QSAR analysis, RSC Adv. 5 (2015) 65153–65166.
[8] B. Vera, K. Vázquez, C. Mascayano, R.A. Tapia, V. Espinosa, J. Soto-Delgado, C. O. Salas, M. Paulino, Structural analysis and molecular docking of trypanocidal aryloxy-quinones in trypanothione and glutathione reductases: a comparison with biochemical data, J. Biomol. Struct. Dyn. 35 (2017) 1785–1803.
[9] G.A. Patani, E.J. LaVoie, Bioisosterism: A rational approach in drug design, Chem. Rev. 96 (1996) 3147–3176.
[10] N.A. Meanwell, Synopsis of some recent tactical application of bioisosteres in drug design, J. Med. Chem. 54 (2011) 2529–2591.
[11] A. Frédéric, A. Ghérardi, P. Nebois, M.-E. Sarciron, A.-F. Pétavy, N. Walchshofer, Benzimidazole-4,7-diones as inhibitors of protozoal (Toxoplasma gondii) purine nucleoside phosphorylase, Bioorg. Med. Chem. Lett. 12 (2002) 977–979.
[12] L. Garuti, M. Roberti, D. Pizzirani, A. Pession, E. Leoncini, V. Cenci, S. Hrelia, Differential antiproliferative activity of new benzimidazole-4,7-diones, Il Farmaco 59 (2004) 663–668.
[13] E. Moriarty, M. Carr, S. Bonham, M.P. Carty, F. Aldabbagh, Synthesis and toxicity towards normal and cancer cell lines of benzimidazolequinones containing fused aromatic rings and 2-aromatic ring substituents, Eur. J. Med. Chem. 45 (2010) 3762–3769.
[14] J.J. Newsome, M.A. Colucci, M. Hassani, H.D. Beall, C.J. Moody, Benzimidazole- and benzothiazole-quinones: excellent substrates for NAD(P)H:quinone oxidoreductase 1, Org. Biomol. Chem. 5 (2007) 3665–3673.
[15] C. Carvalho, D. Siegel, M. Inman, R. Xiong, D. Ross, C.J. Moody, Benzofuranquinones as inhibitors of indoleamine 2,3-dioxygenase (IDO). Synthesis and biological evaluation, Org. Biomol Chem. 12 (2014) 2663–2674.
[16] K. Fahey, L. O'Donovan, M.P. Carty, F. Aldabbagh, The influence of the aziridinyl substituent of benzimidazoles and benzimidazolequinones on toxicity towards normal and Fanconi anaemia cells, Eur. J. Med. Chem. 45 (2010) 1873–1879.
[17] M. Lynch, S. Hehir, P. Kavanagh, D. Leech, J. O'Shaugh-nessy, M.P. Carty, F. Aldabbagh, Synthesis by radical cyclization and cytotoxicity of highly potent bioreductive alicyclic ring fused [1,2-a]benzimidazolequinones, Chem. Eur. J. 13 (2007) 3218–3226.
[18] L. O'Donovan, M.P. Carty, F. Aldabbagh, First synthesis of N-[(aziridin-2-yl) methyl]benzimidazolequinone and analysis of toxicity towards normal and Fanconi anemia cells, Chem. Commun. 5592–5594 (2008).
[19] G. Sliwoski, S. Kothiwale, J. Meiler, E.W., Lowe Jr., Computational methods in drug discovery, Pharmacol. Rev. 66 (2014) 334–395.
[20] L.G. Ferreira, R.N. dos Santos, G. Oliva, A.D. Andricopulo, Molecular docking and structure-based drug design strategies, Molecules 20 (2015) 13384–13421.
[21] S. Pieretti, J.R. Haanstra, M. Mazet, R. Perozzo, C. Bergamini, F. Prati, R. Fato, G. Lenaz, G. Capranico, R. Brun, B.M. Bakker, P.A.M. Michels, L. Scapozza, M. L. Bolognesi, A. Cavalli, Naphthoquinone derivatives exert their antitrypanosomal activity via a multi-target mechanism, PLoS Negl. Trop. Dis. 7 (2013), e2012.
[22] E. Uliassi, G. Fiorani, R.L. Krauth-Siegel, C. Bergamini, R. Fato, G. Bianchini, J. C. Menéndez, M.T. Molina, E. López-Montero, F. Falchi, A. Cavalli, S. Gul, M. Kuzikov, B. Ellinger, G. Witt, C.B. Moraes, L.H. Freitas-Junior, C. Borsari, M. P. Costi, M.L. Bolognesi, Crassiflorone derivatives that inhibit Trypanosoma brucei glyceraldehyde-3-phosphate dehydrogenase (TbGAPDH) and Trypanosoma cruzi trypanothione reductase (TcTR) and display trypanocidal activity, Eur. J. Med Chem. 141 (2017) 138–141.
[23] N. Uchiyama, Z. Kabututu, B.K. Kubata, F. Kiuchi, M. Ito, J. Nakayama-Shimada, T. Aoki, K. Ohkubo, S. Fukuzumi, S.K. Martin, G. Honda, Y. Urade, Antichagasic activity of komaroviquinone is due to generation of reactive oxygen species

catalyzed by *Trypanosoma cruzi* Old Yellow Enzyme, Antimicrob. Agents Chemother. 49 (2005) 5123–5126.
[24] M.T. Murakami, N.C. Rodrigues, L.M. Gava, R.V. Honorato, F. Canduri, L.R. S. Barbosa, G. Oliva, J.C. Borges, Structural studies of the *Trypanosoma cruzi* Old Yellow Enzyme: Insights into enzyme dynamics and specificity, Biophys. Chem. 184 (2013) 44–53.
[25] F. Díaz-Viraqué, M.L. Chiribao, A. Trochine, F. González-Herrera, C. Castillo, A. Liempi, U. Kemmerling, J.D. Maya, C. Robello, Old Yellow Enzyme from Trypanosome cruzi exhibits in vivo prostaglandin F2□ synthase activity and has a key role in parasite infection and drug susceptibility, Front. Immunol. 7 (2018) 456.
[26] K.L. Arienti, A. Brunmark, F.U. Axe, K. McClure, A. Lee, J. Blevit, D.K. Neff, L. Huang, S. Crawford, C.R. Pandit, L. Karlsson, J.G. Breitenbucher, Checkpoint kinase inhibitors: Sar and radioprotective properties of a series of 2-arylbenzimidazoles, J. Med. Chem. 48 (2005) 1873–1885.
[27] Y. Venkateswarlu, S.R. Kumar, P. Leelavathi, Facile and efficient one-pot synthesis of benzimidazoles using lanthanum chloride, Org. Med. Chem. Lett. 3 (2013) 7.
[28] P. Hammershøj, T.K. Reenberg, M. Pittelkow, C.B. Nielsen, O. Hammerich, J. B. Christensen, Synthesis and properties of 2,3-dialkynyl-1,4-benzoquinones, Eur. J. Org. Chem. 2786–2794 (2006).
[29] L. Garuti, M. Roiberti, M. Malagoli, T. Rossi, M. Castelli, Synthesis and antiproliferative activity of some benzimidazole-4,7-dione derivatives, Bioorg. Med. Chem. Lett. 10 (2000) 2193–2195.
[30] T.B. Nguyen, J. Le Bescont, L. Ermolenko, A. Al-Mourabit, Cobalt- and iron-catalyzed redox condensation of *o*-substituted nitrobenzenes with alkylamines: A step- and redox-economical synthesis of diazaheterocycles, Org. Lett. 15 (2013) 6218–6221.
[31] D. Yang, D. Fokas, J. Li, L. Yu, C.M. Baldino, A versatile method for the synthesis of benzimidazoles from *o*-nitroanilines and aldehydes in one step via a reductive cyclization, Synthesis (2005) 47–56.
[32] H. Göker, M. Alp, Z. Ates-Alagöz, S. Yildiz, Synthesis and potent antifungal activity against *Candida* species of some novel 1H-benzimidazoles, J. Heterocycl. Chem. 46 (2009) 936–948.
[33] H. Fan, Y. Li, L. Li, X. Ren, One kind of bibenzoimidazolyl derivatives, their preparation and their use, CN Patent (2015), 1047104410 A.
[34] M.L. Bolognesi, F. Lizzi, R. Perozzo, R. Brun, A. Cavalli, Synthesis of a small library of 2-phenoxy-1,4-naphthoquinone and 2-phenoxy-1,4-anthraquinone derivatives bearing anti-trypanosomal and anti-leishmanial activity. From a multitarget antitrypanosomal to a potential antitumor profile, Bioorg. Med. Chem. Lett. 18 (2008) 2272–2276.
[35] R. Martin-Escolano, E. Moreno-Viguri, M. Santivañez-Veliz, A. Martin-Montes, E. Medina-Carmona, R. Paucar, C. Marín, A. Azqueta, N. Cirauqui, A.L. Pey, S. Pérez-Silanes, M. Sánchez-Moreno, Second generation of Manich base-type derivatives with in vivo activity against Trypanosoma cruzi, J. Med. Chem. 61 (2018) 5643–5663.
[36] R. Don, J.R. Ioset, Screening strategies to identify new chemical diversity for drug development to treat kinetoplastid infections, Parasitology 141 (2014) 140–146.
[37] K.C.G. De Moura, K. Salomao, R.F.S. Menna-Barreto, F.S. Emery, M.C.F.R. Pinto, A. V. Pinto, S.L. de Castro, Studies on the trypanocidal activity of semi-synthetic pyran[*b*-4,3]naphtho[1,2-*d*]imidazoles from β-lapachone, Eur. J. Med. Chem. 39 (2004) 639–645.
[38] C.-K. Ryu, E.-H. Song, J.-Y. Shim, H.-J. You, K.U. Choi, I.H. Choi, E.Y. Lee, M. J. Chae, Synthesis and antifungal activity of 2,5-disubstituted-6-arylamino-4,7-benzimidazolediones, Bioorg. Med. Chem. Lett. 13 (2003) 17–20.
[39] W. Sherman, T. Day, M.P. Jacobson, R.A. Friesner, R. Farid, Novel procedure for modeling ligand/receptor induced fit effects, J. Med. Chem. 49 (2006) 534–553.
[40] F. Belluti, E. Uliassi, G. Veronesi, C. Bergamini, M. Kaiser, R. Brun, A. Viola, R. Fato, P.A.M. Michels, R.L. Krauth-Siegel, A. Cavalli, M.L. Bolognesi, Toward the development of dual-targeted glyceraldehyde-3-phosphate dehydrogenase/trypanothione reductase inhibitors against *Trypanosoma brucei* and *Trypanosoma cruzi*, ChemMedChem 9 (2014) 371–382.
[41] D.H.F. Souza, R.C. Garratt, A.P.U. Araújo, V.G. Guimarães, W.D.P. Jesus, P.A. M. Michels, V. Hannaert, G. Oliva, *Trypanosoma cruzi* glycosomal glyceraldehyde-3-phosphate dehydrogenase: structure, catalytic mechanism and targeted inhibitor design, FEBS Lett. 424 (1998) 131–135.
[42] C. Eberle, B.S. Lauber, D. Fankhauser, M. Kaiser, R. Brun, R.L. Krauth-Siegel, F. Diederich, Improved inhibitors of trypanothione reductase by combination of motifs: Synthesis, Inhibitory potency, binding mode, and antiprotozoal activities, ChemMedChem 6 (2011) 292–301.
[43] B. Stump, C. Eberle, M. Kaiser, R. Brun, R.L. Krauth-Siegel, F. Diederich, Diaryl sulphide-based inhibitors of trypanothione reductase: inhibition potency, revised binding mode and antiprotozoal activities, Org. Biomol. Chem. 6 (2008) 3935–3947.
[44] C. Morin, T. Besset, J.-C. Moutet, M. Fayolle, M. Brückner, D. Limosin, K. Becker, E. Davioud-Charvet, The aza-analogues of 1,4-naphthoquinones are potent substrates and inhibitors of plasmodial thioredoxin and glutathione reductases and of human erythrocyte glutathione reductase, Org. Biomol. Chem. 6 (2008) 2731–2742.
[45] L. Krause, R. Herbst-Irmer, G.M. Sheldrick, D. Stalke, Comparison of silver and molybdenum microfocus X-ray sources for single-crystal structure determination, J. Appl. Cryst. 48 (2015) 3–10.
[46] G.M. Sheldrick, SHELXL-Integrated space-group and crystal determination, Acta Cryst. A71 (2015) 3–8.
[47] G.M. Sheldrick, Crystal structure refinement with SHELXL, Acta Cryst. C 71 (2015) 3–8.
[48] M. Vieites, L. Otero, D. Santos, C. Olea-Azar, E. Norambuena, G. Aguirre, H. Cerecetto, M. González, U. Kemmerling, A. Morello, J.D. Maya, D. Gambino, Platinum-based complexes of bioactive 3-(5-nitrofuryl)acroleine thiosemicarbazones showing anti-*Trypanosoma cruzi* activity, J. Inorg. Biochem. 103 (2009) 411–418.
[49] M. Faundez, L. Pino, P. Letelier, C. Ortiz, R. López, C. Seguel, J. Ferreira, M. Pavani, A. Morello, J.D. Maya, Buthionine sulfoximine increases the toxicity of nifurtimox and benznidazole to *Trypanosoma cruzi*, Antimicrob. Agents Chemother. 49 (2005) 126–130.
[50] C.S. Bond, Y. Zhang, M. Berriman, M.L. Cunningham, A.H. Fairlamb, W.N. Hunter, Crystal structure of Trypanosoma cruzi trypanothione reductase in complex with trypanothione, and the structure-based discovery of new natural product inhibitors, Structure 7 (1999) 81–89.
[51] F. Pavao, M.S. Castilho, M.T. Pupo, R.L. Dias, A.G. Correa, J.B. Fernandes, M.F. da Silva, J. Mafezoli, P.C. Vieira, G. Oliva, Structure of Trypanosoma cruzi glycosomal glyceraldehyde-3-phosphate dehydrogenase complexed with chalepin, a natural product inhibitor, at 1.95 A resolution, FEBS Lett. 520 (2002) 13–17.
[52] N. Okamoto, K. Yamaguchi, E. Mizohata, K. Tokuoka, N. Uchiyama, S. Sugiyama, H. Matsumura, K. Inaka, Y. Urade, Y.T. Inoue, Structural insight into the stereoselective production of PGF2(alpha) by Old Yellow Enzyme from *Trypanosoma cruzi*, J. Biochem. 150 (2011) 563–568.
[53] L.L.C. Schrödinger, Schrödinger Release 2018–4: Schrödinger Suite 2018–4 Protein Preparation Wizard; Epik, Schrödinger LLC, New York, NY; Impact, Prime, Schrödinger, LLC, New York, NY, USA, 2018.
[54] L.L.C. Schrödinger, Schrödinger Release 2018–4: LigPrep, Schrödinger LLC, New York, NY, USA, 2018.
[55] M.R. Gunner, T. Murakami, A.S. Rustenburg, M. Isik, J.D. Chodera, Standard state free energies, not pKas, are ideal for describing small molecule protonation and tautomeric states, J. Comput. Aided Mol. Des. 34 (2020) 561–573.
[56] R.A. Friesner, R.B. Murphy, M.P. Repasky, L.L. Frye, J.R. Greenwood, T.A. Halgren, P.C. Sanschagrin, D.T. Mainz, Extra precision glide: Docking and scoring incorporating a model of hydrophobic enclosure for protein−ligand complexes, J. Med. Chem. 49 (2006) 6177–6196.
[57] S. Salentin, S. Schreiber, V.J. Haupt, M.F. Adasme, M. Schroeder, M. PLIP: fully automated protein–ligand interaction profiler, Nucleic Acids Res. 43 (2015) W443–W447.
[58] W.L. DeLano, Pymol: an open-source molecular graphics tool. CCP4 Newsletter on protein crystallography, Science 40 (2002) 82–92.